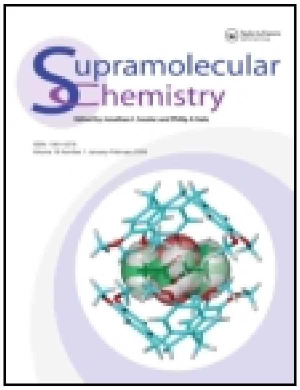

Supramolecular Chemistry
Publication details, including instructions for authors and subscription information:
http://www.tandfonline.com/loi/gsch20

Dynamically capped rotaxanes: metal coordination vs. acid-base pairing in the chiral end-capping

Satoshi Shinoda [a] [b] , Takayuki Maeda [a] , Hiroyuki Miyake [a] & Hiroshi Tsukube [a] [b]
[a] Department of Chemistry, Graduate School of Science, Osaka City University, Sugimoto, Sumiyoshi-ku, Osaka, 558-8585, Japan
[b] JST, CREST, Osaka City University, Sugimoto, Sumiyoshi-ku, Osaka, 558-8585, Japan

To cite this article: Satoshi Shinoda, Takayuki Maeda, Hiroyuki Miyake & Hiroshi Tsukube (2011): Dynamically capped rotaxanes: metal coordination vs. acid-base pairing in the chiral end-capping, Supramolecular Chemistry, 23:03-04, 244-248

To link to this article: http://dx.doi.org/10.1080/10610278.2010.521838

Supramolecular Chemistry
Vol. 23, Nos. 3–4, March–April 2011, 244–248

Taylor & Francis
Taylor & Francis Group

Dynamically capped rotaxanes: metal coordination vs. acid–base pairing in the chiral end-capping

Satoshi Shinoda[ab]*, Takayuki Maeda[a], Hiroyuki Miyake[a] and Hiroshi Tsukube[ab]

[a]*Department of Chemistry, Graduate School of Science, Osaka City University, Sugimoto, Sumiyoshi-ku, Osaka 558-8585, Japan;* [b]*JST, CREST, Osaka City University, Sugimoto, Sumiyoshi-ku, Osaka 558-8585, Japan*

(*Received 9 July 2010; final version received 15 August 2010*)

A series of pseudorotaxanes were formed by mixing a thread molecule and several crown ethers. Crystal structure analysis clearly indicated that hydrogen bonding between NH_2^+ of the thread molecule and crown ether oxygen atoms was significantly involved, together with cation–dipole interactions between cationic nitrogen and ether oxygen atoms. End-capping of the pseudorotaxane with chiral metal complexes gave dynamically capped rotaxanes including dibenzo-24-crown-8. This exhibited induced circular dichroism signals around the benzo-crown and anthracene-thread chromophore regions, while a chiral organic acid formed rotaxane exhibiting weaker signals.

Keywords: rotaxane; dynamic capping; chirality; metal coordination; acid–base pairing

Introduction

Rotaxanes are a family of the most sophisticated molecules in the field of supramolecular chemistry, and are applicable in the design of molecular shuttles, switches and other functional machines (*1*). Since their original construction, which composed of a thread, a wheel and capping moieties, a variety of combinations have been employed to design rotaxanes exhibiting characteristic structures and functions at the molecular level. There are two typical examples of rotaxanes, those connected with capping groups via covalent bonds and those connected via non-covalent bonds (Figure 1) (*2*). Covalent bond formation has traditionally been employed to link the thread molecule with the end-capping group. Although various functional molecules were incorporated in the rotaxane frameworks, the wheel molecules usually remained at the original positions to exhibit static properties. On the other hand, dynamically capped rotaxanes have been prepared using non-covalent bonds, in which the wheels rapidly exchanged between the inserted and free forms. Metal complexes are particularly useful as dynamic end-capping reagents (*3*), and Cu^{2+} ions, Pt complexes or Ru complexes have been used as part of rotaxane frameworks (*4*). Here, we report the synthesis of pseudorotaxanes from a new thread molecule and its dynamic capping properties. A chiral metal complex and an organic acid were selected as capping agents in order to compare metal coordination and acid–base pairing. Chiral-capped rotaxanes were applied in asymmetric catalysis and other chiral processes (*5*), some of which formed stable and dynamic rotaxanes exhibiting interesting chiroptical behaviours. The present study indicates that further combinations of chiral metal complexes and the designed pseudorotaxanes will provide a new series of rotaxane-based functional materials.

Results and discussion

Pseudorotaxane formation

We chose thread molecule **1**, which includes sterically bulky anthracene and a pyridine ring as the end groups: the former acts as an intense chromophore in fluorescence and circular dichroism (CD) spectroscopies. The latter provides metal coordination and acid–base interaction. Furthermore, thread **1** contains a secondary ammonium cation ($-NH_2^+-$) in the middle of the chain, which can interact with crown ethers. Figure 2 summarises the structures of thread **1**, crown ethers **2**–**5** and capping reagents **6** and **7**. As molecular wheels, 24-crown-8 derivatives often interact with thread molecules having secondary ammonium cations as binding sites (*6*). We compared crown ethers having different ring sizes such as 21-, 24-, 27- and 30-membered rings in the pseudorotaxane synthesis (*7*). The pseudorotaxane formation was followed by NMR, ESI-MS and crystal structure determination methods. When thread **1** and 24-crown-8 **3a** were mixed in CD_3CN, separate signals for the methylene protons adjacent to the anthracene unit of thread **1** were detected at δ 5.52 ppm (complex form) and 5.25 ppm (free form), which could be used to estimate the yields of the pseudorotaxane. ESI-MS experiments also

---

*Corresponding author. Email: shinodas@sci.osaka-cu.ac.jp

ISSN 1061-0278 print/ISSN 1029-0478 online

DOI: 10.1080/10610278.2010.521838
http://www.informaworld.com

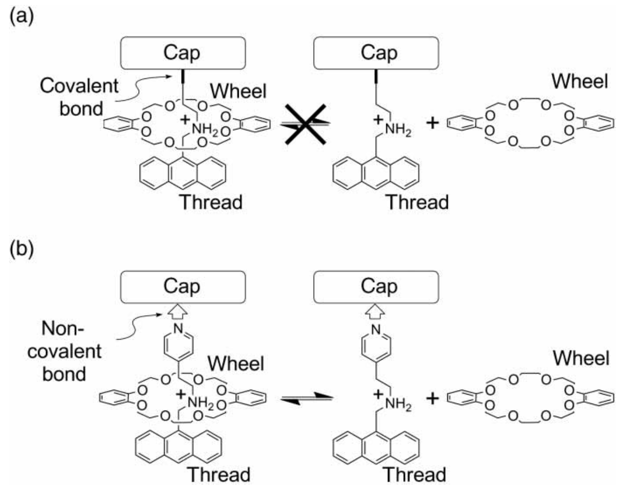

Figure 1. Static and dynamic rotaxanes via covalent and non-covalent bonds, respectively.

revealed the formation of the pseudorotaxane (calculated for $[\mathbf{1} + \mathbf{3a} - \mathrm{PF}_6]^+ = 761.4$ and observed for $m/z = 761.7$).

Figure 3 illustrates the crystal structure of pseudorotaxane **1**–**3a**, in which the molecular chain of thread **1** was inserted into the cavity of the 24-crown-8 ring. As reported earlier (*8*), two hydrogen bonds were formed between the secondary ammonium hydrogen and benzo-oxygen atoms, and cation–dipole interactions were also found to stabilise the pseudorotaxane structure: $[\mathrm{N}^+\cdots\mathrm{O}]$ distances (Å) = 2.99 (a), 2.97 (b), 2.94 (c), 3.20, 3.69, 4.15, 4.36 and 4.17.[1] The distances relating to hydrogen bonds are very close to the reported values 3.01, 3.04 and 2.98 Å, respectively (*8*).

Table 1 summarises the yields of pseudorotaxanes with various crown ethers as determined by NMR spectroscopy. Among the 24-crown-8s **3a**–**3c**, dibenzo- and unsubstituted derivatives, **3a** and **3c** formed the stable pseudorotaxanes (45 and 61%) under the employed conditions, while the dicyclohexyl **3b** gave only a small amount of the product (11%). Dibenzo-24-crown-8 **3a** exhibited a higher yield (45%) than the corresponding 27- and 30-membered crown ethers, **4a** (22%) and **5a** (13%). Since 21-crown-7 **2a** did not give the pseudorotaxane (0%), ring-size effects were found to play a significant role in the present pseudorotaxane synthesis.

Rotaxane formation by end-capping with metal complexes

End-capping of pseudorotaxanes including 24-crown-8s, **3a** and **3c**, was performed with metal complexes **6** or chiral sulphonic acid **7** via two routes in $\mathrm{CD_3CN/CDCl_3}$ (3/7, v/v) (Table 2). Under the employed conditions, pseudorotaxanes were quantitatively formed (>99%) in each case. The pseudorotaxane was reacted with a capping reagent in route A, while 24-crown-8 was added after the reaction between thread **1** and the capping reagent in route B. If the crown ether exchanged only minimally between the

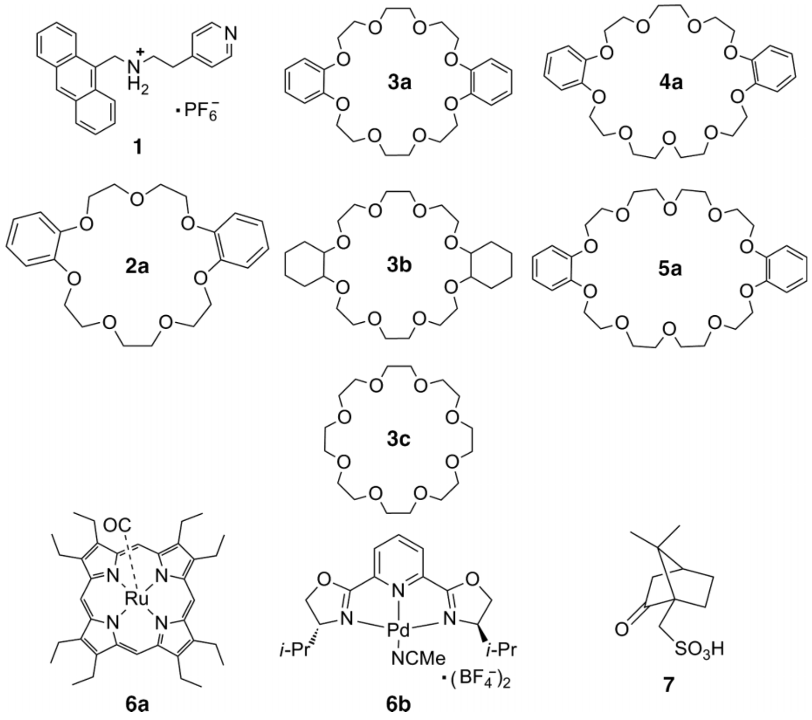

Figure 2. Structures of thread **1**, crown ethers **2**–**5** and capping reagents **6** and **7**.

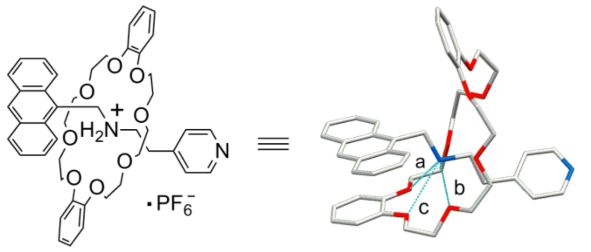

Figure 3. Crystal structure of pseudorotaxane **1–3a**. [$N^{+}\cdots O$] distances are (a) 2.99 Å, (b) 2.97 Å and (c) 2.94 Å.

inserted and free forms, the rotaxane was produced only via route A. The reaction process of pseudorotaxane composed of **1** and **3a** with metal complexes **6a** and **6b** was followed by NMR and ESI-MS methods. When **1** and **3a** formed a pseudorotaxane, it showed a pyridine H-3 signal at δ 6.61 ppm. Upon addition of Ru porphyrin **6a**, this signal was shifted significantly to δ 0.45 ppm, indicating pyridine coordination to **6a** and ring current effects of the porphyrin. When Pd complex **6b** (*9*) was used as a capping reagent, the pyridine H-3 signal appeared at δ 7.20 ppm, which is also a good indication of pyridine coordination to Pd complex **6b**. The observed MS values for the resulting rotaxanes are identical to those of the calculated values: $m/z = 1423.6$ for $[\mathbf{1} + \mathbf{3a} + \mathbf{6a} - \mathrm{PF_6}]^{+}$; 1400.4 for $[\mathbf{1} + \mathbf{3a} + \mathbf{6b} - \mathrm{PF_6}]^{+}$; 994.0 for $[\mathbf{1} + \mathbf{3a} + \mathbf{7} - \mathrm{PF_6}]^{+}$. Table 2 shows the obtained rotaxanes with metal complexes **6a** and **6b** determined by the integration of the pyridine H-2 signals. Both routes A and B for each combination gave similarly high yields (81–93%), indicating that the capping had minimal influence on the crown ether exchange process. The thread molecule was rapidly inserted in and out of the crown ether ring, but the exchange rate was slower than the NMR timescale as distinct proton signals for the crown ether appeared for the free and complexed forms.[2] When chiral sulphonic acid **7** was employed as the chiral capping reagent (*10*), proton signals of the pyridine ring shifted downfield, indicating that sulphonic acid **7** readily formed an acid–base pair with the pyridine end group of thread **1**. As a gradual shift of the pyridine protons was observed when increasing the amount of **7** ([**7**]/[pseudorotaxane] < 1), it was clear that acid–base pairing provided more dynamic properties than metal coordination.

Table 1. Synthesis of pseudorotaxanes with various crown ethers.

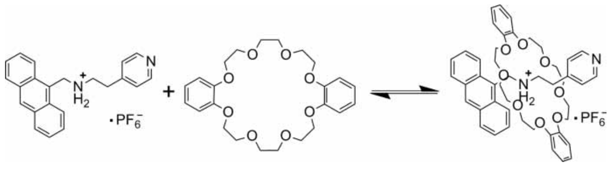

Crown ether	Yield (%)	ESI-MS observed/calculated
2a	0	–/–
3a	45	761.7/761.4
3b	11	773.4/773.2
3c	61	665.4/665.7
4a	22	805.7/805.7
5a	13	849.8/849.5

Note: [**1**] = [crown ether] = 2.0×10^{-3} M in CD_3CN.

Table 2. Synthesis of rotaxanes with crown ethers **3a** and **3c** and capping reagents **6a** and **6b**.

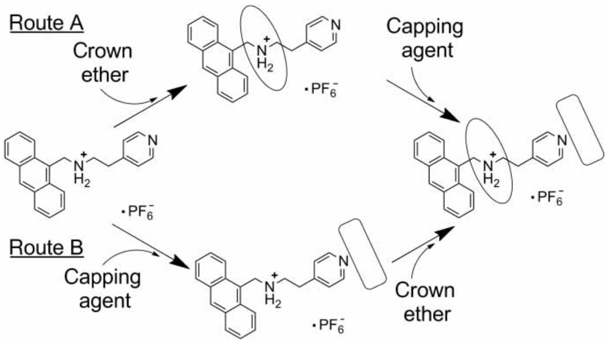

		Yield of rotaxane (%)				
		3a		**3c**		
		1 h	24 h	1 h	24 h	No crown ether
6a	Route A	81	82	84	84	77
	Route B	82	81	83	83	
6b	Route A	93	91	87	85	84
	Route B	91	88	85	87	

Notes: [**1**] = [**6**] = 5.0×10^{-4} M, [**3**] = 1.0×10^{-2} M in $CD_3CN/CDCl_3$ (3/7, v/v). Experiments were performed by two routes. Route A: first, **1** and crown ether were mixed and then **6** was added. Route B: **1** and **6** were mixed and then crown ether was added. ^{1}H NMR spectra were measured after 1 and 24 h to determine the yield of the rotaxane. In the absence of crown ether, NMR spectra were measured after 1 h.

When chiral metal complex **6b** reacted with thread **1** in the absence of crown ether at −20°C, the induced CD signals appeared around 320–400 nm upon metal coordination. As shown in Figure 4(a), difference spectra between [thread **1** + Pd complex] and [pyridine + Pd complex] showed CD signals at the absorption bands of anthracene (350–400 nm). Further addition of dibenzo-crown ether **3a** (Figure 4(a)) slightly decreased the CD signals at 350–400 nm but induced new CD signals around the benzo-chromophore region (<280 nm). These observations revealed that chirality induction occurred through two kinds of non-covalent bonds such as metal coordination and crown interaction. In other words, chiral metal complexes added chiroptical properties to both wheel and thread molecules of the rotaxane. At present, we do not have any insights into the asymmetric induction. When chiral sulphonic acid **7** reacted

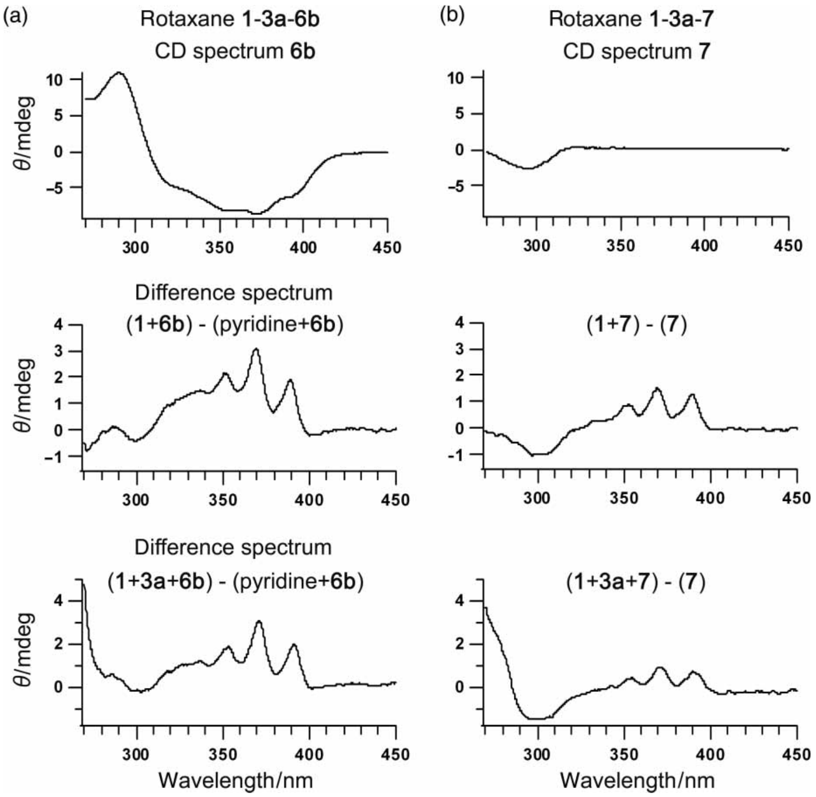

Figure 4. CD characterisations of rotaxanes at − 20 °C. [**1** or pyridine] = 6.0 × 10^{-4} M, [**3b**] = 1.2 × 10^{-3} M and [**6** or **7**] = 6.0 × 10^{-4} M. $CH_3CN/CHCl_3$ (3/7, v/v). Ellipticity was measured in a 0.1 cm quartz cell.

with thread **1** in the absence of crown ether (Figure 4(b)), the induced CD signals appeared, but the intensity was half that of the corresponding signals with Pd complex **6a** and addition of crown ether **3a** decreased the intensity of the signals. A metal complex capping reagent was more effective in adding chiroptical features to the rotaxanes (*11*). We only evaluated the strength of asymmetric induction by the intensity of the induced CD signals. In this manner, the effect of camphor sulphonic acid was smaller than that of the Pd complex.

In conclusion, we prepared a series of pseudorotaxanes by mixing a thread molecule and several crown ethers. Chiral metal complex **6b** capped the pseudorotaxanes with 24-crown-8s to provide dynamic capping, and chirality on the wheel and thread molecules was induced. In addition to a chiral capping reagent using acid–base pairing, metal coordination provided a new synthetic method of rotaxanes having dynamic and chiroptical properties.

Experimental section

Materials and compounds

All materials except for **1** and **6b** were purchased and used without further purification.

Anthracen-9-yl-methyl-(2-pyridylethyl)-ammonium hexafluorophosphate (**1**) was synthesised from 9-anthracenecarbaldehyde and 4-(2-aminoethyl)pyridine according to the literature (*8*).

Compound **1**. Yield 32%; mp 215–217°C; ^{1}H NMR (300 MHz, CD_3CN): $\delta = 3.02$ (t, 2H, $J = 7.9$ Hz, NH_2-CH_2CH_2), 3.53 (t, 2H, $J = 7.9$ Hz, $NH_2CH_2CH_2$), 5.27 (s, 2H, $CH_2NH_2CH_2CH_2$), 7.24 (t, 2H, $J = 5.8$ Hz, Py H-3), 7.58–7.64 (m, 4H, anthracene), 7.69–7.75 (m, 2H, anthracene), 8.17 (t, 2H, $J = 8.6$ Hz, anthracene), 8.31 (t, 2H, $J = 8.8$ Hz, anthracene), 8.52 (d, 2H, $J = 5.8$ Hz, Py H-2) and 8.75 (s, 1H, anthracene H-10); IR (KBr) ν: 3605, 3415, 2779, 1614, 1450, 1426, 843, 736 and 559 cm^{-1}; MS (ESI, pos) Calcd for $[M - PF_6^-]^+$; 313.17, Found: 313.3; Anal. Calcd (%) for $C_{22}H_{21}F_6N_2P \cdot 2H_2O$: C, 53.34; H, 5.29; N, 5.65; F, 23.06; Cl, 0.00, Found: C, 53.41; H, 5.12; N, 5.62; F, 23.20; Cl, 0.00.

2,6-Bis[(*R*)-4′-isopropyloxazolin-2′-yl]pyridine palladium(II) acetonitrile (**6b**) was synthesised by the reported method (*9*).

Compound **6b**. Yield 44%; ^{1}H NMR (400 MHz, CD_3CN): $\delta = 8.56$ (t, 1H, $J = 8.2$ Hz, H_{py}), 8.08 (d, 2H, $J = 8.03$ Hz, H_{py}), 5.05–4.95 (m, 4H, H_{ox}), 4.43–4.38 (m, 2H, H_{ox}), 2.13–2.08 (m, 2H, H_{ox}), 1.95 (s, 3H, acetonitrile) and 0.97 (dd, 12H, $J = 7.0$ Hz, H_{Me}); Anal. Calcd (%) for $C_{19}H_{26}B_2F_8N_4O_2Pd$: C, 36.66; H, 4.21; N, 9.00, Found: C, 36.69; H, 4.24; N, 9.08.

Spectroscopic measurements

UV–vis absorption spectra were measured on a JASCO-V670 in a 0.1 cm quartz cell. CD was measured in a 1 mm cell at −20°C on a JASCO-J820 spectrometer with a liquid N_2 cooled temperature controller. ^{1}H NMR measurements were performed on a Jeol LA-400 (400 MHz).

Crystal structure analysis

X-ray diffraction data were collected on a colourless crystal of pseudorotaxane **1–3a** [$(C_{22}H_{21}N_2) \subset (C_{24}H_{32}O_8)$, $(C_{22}H_{22}N_2) \subset (C_{24}H_{32}O_8)$, $(PF_6)_3(CH_3CN)(H_2O)_{3.25}$] of $0.40 \times 0.40 \times 0.10$ mm by a Rigaku/MSC Mercury CCD diffractometer with graphite monochromated Mo Kα radiation ($\lambda = 0.71070$ Å) to $2\theta_{\max}$ of 55.0°. Data were processed on a PC using CrystalClear software (Rigaku). The crystal structures were solved by direct methods using Sir-97 (*12*) and refined by full-matrix least squares on F^2 using SHELX-97 (*13*). All hydrogen atoms except for those in amine moieties were placed on ideally geometrical positions. Non-hydrogen atoms were refined anisotropically. Detailed crystallographic data can be obtained free of charge from The Cambridge Crystallographic Data Centre via www.ccdc.cam.ac.uk/data_request/cif (CCDC-782851).

Acknowledgements

This research was partially supported by Osaka City University and a Core Research for Evolution, Science, and Technology (CREST) programme grant from the Japan Science and Technology (JST) Agency.

Notes

1. X-ray data for [$(C_{22}H_{21}N_2) \subset (C_{24}H_{32}O_8)$, $(C_{22}H_{22}N_2) \subset (C_{24}H_{32}O_8)$, $(PF_6)_3(CH_3CN)(H_2O)_{3.25}$]: formula = $C_{94}H_{116.5}F_{18}N_5O_{19.25}P_3$, $M_r = 2059.33$, triclinic, space group $P\bar{1}$, $a = 14.4617(19)$ Å, $b = 15.691(2)$ Å, $c = 24.651(3)$ Å, $\alpha = 99.434(4)°$, $\beta = 99.141(2)°$, $\gamma = 112.592(5)°$, $V = 4941.2(11)$ Å^3, $Z = 2$, $\rho_{\text{calcd}} = 1.384\ \text{g cm}^{-3}$, $\mu = 0.163\ \text{mm}^{-1}$, $T = 100(2)$ K, $F(000) = 2153$, 38,067 reflections collected, of which 21,332 unique reflection were used ($R_{\text{int}} = 0.0457$). Final R indices [21,332 observed reflections, $I > 2\sigma(I)$]: $R_1 = 0.1137$, $wR_2 = 0.2355$. GOF = 1.143. Highest residual electron density 0.836 e Å^{-3}
2. The binding constants (log K) of thread **1** with benzo-24-crown-8 **3a** and metal complexes **6a** and **6b** were determined in $CD_3CN/CDCl_3$ (3/7, v/v) at 25°C by the integration ratio of the ^{1}H NMR signals: **1–3a**, 4.2 ± 0.1; **1–6a**, 4.5 ± 0.1; **1–6b**, 4.8 ± 0.1. We did not determine the precise exchange rate constants for these complexation processes.

References

(1) (a) Saha, S.; Stoddart, J.F. *Chem. Soc. Rev.* **2007**, *36*, 77–92. (b) Loeb, S.J. *Chem. Soc. Rev.* **2007**, *36*, 226–235. (c) Makita, Y.; Kihara, N.; Takata, T. *J. Org. Chem.* **2008**, *73*, 9245–9250.

(2) Dynamic covalent bonds such as disulphide and imine were also effectively used in the rotaxane formation. (a) Furusho, Y.; Hasegawa, T.; Tsuboi, A.; Kihara, N.; Takata, T. *Chem. Lett.* **2000**, 18–19. (b) Kawai, H.; Umehara, T.; Fujiwara, K.; Tsuji, T.; Suzuki, T. *Angew. Chem. Int. Ed.* **2006**, *45*, 4281–4286. (c) Umehara, T.; Kawai, H.; Fujiwara, K.; Suzuki, T.J. *Am. Chem. Soc.* **2008**, *130*, 13981–13988.

(3) Suzaki, Y.; Taira, T.; Osakada, K.; Horie, M. *Dalton Trans.* **2008**, *36*, 4823–4833.

(4) (a) Knight, L.K.; Vukotic, V.N.; Viljoen, E.; Caputo, C.B.; Loeb, S.J. *Chem. Commun.* **2009**, 5585–5587. (b) Suzaki, Y.; Osakada, K. *Chem. Asian. J.* **2006**, *1*, 331–343. (c) Chichak, K.; Walsh, M.C.; Branda, N.R. *Chem. Commun.* **2000**, 847–848.

(5) (a) Tachibana, Y.; Kihara, N.; Takata, T. *J. Am. Chem. Soc.* **2004**, *126*, 3438–3439. (b) Lee, A.L. *Annu. Rep. Prog. Chem. B.* **2009**, *105*, 421–439. (c) Kameta, N.; Nagawa, Y.; Karikomi, M.; Hiratani, K. *Chem. Commun.* **2006**, 3714–3716.

(6) Ashton, P.R.; Baxter, I.; Fyfe, M.C.T.; Raymo, F.M.; Spencer, N.; Stoddart, J.F.; White, A.J.P.; Williams, D.J. *J. Am. Chem. Soc.* **1998**, *120*, 2297–2307.

(7) Effect of crown ether ring size on the stability constant of pseudorotaxane has been studied: (a) Tokunaga, Y.; Yoshioka, M.; Nakamura, T.; Goda, T.; Nakata, R.; Kakuchi, S.; Shimomura, Y. *Bull. Chem. Soc. Jpn.* **2007**, *80*, 1377–1382. (b) Hirose, K.; Shiba, Y.; Ishibashi, K.; Doi, Y.; Tobe, Y. *Chem. Eur. J.* **2008**, *14*, 981–986.

(8) Ashton, P.R.; Ballardini, R.; Balzani, V.; Gómez-López, M.; Lawrence, S.E.; Martínez-Díaz, M.V.; Montalti, M.; Piersanti, A.; Prodi, L.; Stoddart, J.F.; Williams, D.J. *J. Am. Chem. Soc.* **1997**, *119*, 10641–10651.

(9) Moriuchi, T.; Shen, X.; Hirao, T. *Tetrahedron* **2006**, *62*, 12237–12246.

(10) Barrett, R.; Caine, D.M.; Cardwell, K.S.; Cooke, J.W.B.; Lawrence, R.M.; Scott, P.; Sjolin, Å. *Tetrahedron Asymmetry* **2003**, *14*, 3627–3631.

(11) (a) Bottari, G.; Leigh, D.A.; Pérez, E.M. *J. Am. Chem. Soc.* **2003**, *125*, 13360–13361. (b) Kiahan, M. R.; Parham, A.; Schelhase, F.; Yoneva, A.; Silva, G.; Chen, X.; Okamoto, Y.; Vögtle, F. *Angew. Chem. Int. Ed.* **2006**, *45*, 7296–7299.

(12) Altomare, A.; Burla, M.C.; Camalli, M.; Cascarano, G.; Giacovazzo, C.; Guagliardi, A.; Moliterni, A.G.G.; Polidori, G.; Spagna, R. *J. Appl. Cryst.* **1999**, *32*, 115–119.

(13) Sheldrick, G.M. *SHELX-97*; University of Göttingen: Göttingen, Germany, 1997.